

**Study on formulation to improve
pharmacokinetics of extracellular vesicles
based on their physicochemical properties**

(要約版)

2023

Yuki Kobayashi

Preface

Extracellular vesicles (EVs) are nano-sized membranous vesicle released by various types of cells [1–4]. It is reported that secreted EVs from donor cells contain miRNA and proteins derived from that cell and function as intercellular communication tools by delivering their cargos to the recipient cells[3,5] EVs have advantages on high biocompatibility, utilization of endogenous function and easily genetic engineering [6]. Therefore, EVs are expected for a novel drug delivery system (DDS). However, EVs are heterogenous vesicles that have different physicochemical properties (*e.g.* size and surface charge) and biomolecules composition [7,8]. EV subpopulation can show different pharmacokinetic properties depend on their physicochemical and biological properties.

The improvement of EV productivity and pharmacokinetics (PK) is an important issue for EV-based formulation [9]. As for PK of EVs, researchers have revealed that intravenously administered small EVs (sEVs) rapidly eliminated by macrophages because of recognition of charge of EVs [10,11]. Recently, our laboratory reported a novel sEV subpopulation with a long blood circulation, while the productivity of this subpopulation was limited [12]. Therefore, first of all, I decided to increase productivity of the target EV subpopulation for EV-based formulation.

Oral administration is a non-invasive administration route and is easy for patients. To date, application for oral administration of various nanoparticles for effective drug delivery has been reported on their PK and therapeutic effects [13,14]. Compared to PK of EVs in blood, there was less information on PK of EVs in gastrointestinal tract (GI). Therefore, investigation of PK of EVs can be useful for developing oral EV formulation. In addition, the size of nanoparticles can be one of important factors for the improvement of absorption because of the smaller size can show higher permeability [13,15]. Therefore, the size of EVs can also affect on PK profile of EVs.

Thus, in this thesis, I attempted to develop methods for improving the productivity of target EV subpopulation and for qualitatively detecting them, which can be useful for the development of EV-based formulation. Moreover, I investigated the effect of size of EV PK and on permeability in GI tract.

Table of Contents

Preface	1
Table of Contents	2
Chapter 1	4
1. INTRODUCTION	5
SECTION 1	6
1.1.1. Introduction	6
1.1.2. Materials and Methods	6
<i>1.1.2.1. Cell culture</i>	<i>6</i>
<i>1.1.2.2. Animals</i>	<i>7</i>
<i>1.1.2.3. Plasmid DNA (pDNA)</i>	<i>7</i>
<i>1.1.2.4. sEV isolation from culture medium</i>	<i>7</i>
<i>1.1.2.5. Preparation of PSD or L7Ae protein</i>	<i>7</i>
<i>1.1.2.6. Characterization of PSD protein composition</i>	<i>8</i>
<i>1.1.2.7. Liposome preparation</i>	<i>8</i>
<i>1.1.2.8. Flow cytometry assay</i>	<i>8</i>
<i>1.1.2.9. Treatment of sEVs with PSD or L7Ae</i>	<i>8</i>
<i>1.1.2.10. Characterization of physicochemical properties of sEVs</i>	<i>9</i>
<i>1.1.2.11. Affinity capture of PS⁽⁺⁾ sEVs using TIM4-conjugated beads</i>	<i>9</i>
<i>1.1.2.12. Blood clearance</i>	<i>9</i>
<i>1.1.2.13. Statistical analysis</i>	<i>9</i>
1.1.3. Results	9
<i>1.1.3.1. PSD-coding pDNA was constructed and PSD protein was successfully purified</i>	<i>9</i>
<i>1.1.3.2. Purified PSD protein exhibited enzyme activity</i>	<i>11</i>
<i>1.1.3.3. PSD-treated sEVs were identified as PS⁽⁻⁾ sEV-enriched subpopulation</i>	<i>12</i>
<i>1.1.3.4. PS⁽⁻⁾ sEVs recovered from PSD-treated bulk sEVs showed long blood-circulation periods</i>	<i>14</i>
1.1.4. Discussion	15
1.1.5. Summary of Section 1	16
SECTION 2	17
Chapter 2	19
Conclusion	22
List of publications included in this thesis	23

Acknowledgements	24
References.....	25

Chapter 1

**Improvement of productivity and
development of detection methods for PS
low expression
small extracellular vesicles**

1. Introduction

Small extracellular vesicles (sEVs), EVs with diameters of approximately 100 nm, is the most popular EV population. It has been reported that bulk sEVs isolated from cell culture medium using ultracentrifugation are rapidly cleared from blood circulation with an elimination half-life ($t_{1/2\alpha}$) of less than 10 min and taken up mainly by macrophages in the liver after intravenous injection [11,16,17]. On the other hand, a minor subpopulation of sEVs, phosphatidylserine (PS)-deficient sEVs ($PS^{(-)}$ sEVs), which can be isolated from bulk sEVs, shows prolonged circulation [12]. Therefore, $PS^{(-)}$ sEVs are attractive candidate for drug delivery systems. However, limited productivity of $PS^{(-)}$ sEVs and lack in a method to perform qualitative analysis of $PS^{(-)}$ sEVs makes it difficult for the development of $PS^{(-)}$ sEVs-based formulation for delivery systems.

In chapter 1, I focused on charge of sEVs, and aiming to increase the productivity of $PS^{(-)}$ sEVs subpopulations and to develop a labeling method for detecting sEVs to check the quality of sEVs for $PS^{(-)}$ sEV-based formulation.

Section 1

Preparation of small extracellular vesicles (sEVs) with low PS expression by enzymatic treatment to improve productivity of sEVs with high blood retention

1.1.1. Introduction

In previous studies, the key molecules that are responsible for the rapid clearance of sEVs in blood were identified and discovered a novel sEV subpopulation with a long $t_{1/2\alpha}$ [11,12,17,18]. Phosphatidylserine (PS) is a negatively charged phospholipid that is abundant in sEV membranes [19,20]. The negative charge derived from PS in sEVs has been found to play a crucial role in their recognition and uptake by macrophages [11,21]. In addition, sEVs with less PS exposed on their outer membranes, PS⁽⁻⁾ sEVs were isolated from bulk sEVs and identified as an sEV subpopulation with an extremely long blood retention time [12]. Although PS⁽⁻⁾ sEVs were a minor sEV subpopulation that constituted approximately 10% of the bulk sEV population [12], the rate of their yield from bulk sEVs, which is considered insufficient for therapeutic applications. Therefore, the development of efficient preparation methods for PS⁽⁻⁾ sEVs remains a challenging issue.

In this section, to increase the yield of PS⁽⁻⁾ sEVs from bulk sEVs I used phosphatidylserine decarboxylase (PSD), a mitochondrial enzyme that converts PS into phosphatidylethanolamine (PE) [22]. I hypothesized PSD treatment depletes PS on bulk sEV surfaces, leading in an increase of PS⁽⁻⁾ sEVs. I performed PSD treatment of bulk sEVs to increase the yield of PS⁽⁻⁾ sEVs and subsequently evaluated the physicochemical and pharmacokinetic properties of sEVs treated with PSD.

1.1.2. Materials and Methods

1.1.2.1. Cell culture

Murine melanoma (B16-BL6) cells were obtained from Riken BRC (Japan) and cultured in Dulbecco's modified Eagle medium (Nissui Pharmaceutical, Japan) supplemented with 10% heat-inactivated fetal bovine serum and penicillin/streptomycin/L-glutamine (Nacalai Tesque, Japan) at 37°C under humidified air containing 5% CO₂.

1.1.2.2. Animals

Five-week-old male BALB/c mice were purchased from Japan SLC, Inc. (Japan). All protocols for the animal experiments were approved by the Animal Experimentation Committee of the Graduate School of Pharmaceutical Sciences of Kyoto University.

1.1.2.3. Plasmid DNA (pDNA)

The pDNA encoding gLuc-Lamp2c was constructed as previously reported [12,16]. Briefly, for vector construction, the promoter and enhancer coding sequences of the pCpG-mcs vector (Thermo Fisher Scientific, USA) were amplified by PCR and subcloned into the SmaI and HindIII sites of pBROAD2-mcs (InvivoGen, USA). The chimeric sequence of gLuc-Lamp2c was subcloned into the AflIII and KpnI sites of the constructed vector.

1.1.2.4. sEV isolation from culture medium

B16-BL6 cells were transfected with pDNA using polyethylenimine “Max” (Polysciences, USA) as described previously [23]. After the transfection, the medium was replaced with Opti-MEM (Thermo Fisher Scientific) and cultured for 24 h. Next, the conditioned medium was collected and subjected to sequential centrifugation ($300 \times g$ for 10 min, $2,000 \times g$ for 20 min, and $10,000 \times g$ for 30 min), to remove cellular debris and large vesicles, followed by filtration through a 0.2 μm filter. The filtered medium was then ultra-centrifuged twice at $100,000 \times g$ for 1 h. The pellet was washed with phosphate-buffered saline (PBS) and spun again at $100,000 \times g$ for 1 h. The sEV pellet was re-suspended in PBS, and the amount of recovered sEVs was estimated by measuring the protein concentration using the Bradford assay [23].

1.1.2.5. Preparation of PSD or L7Ae protein

PSD and FLAG (DYKDDDDK) coding sequences were synthesized by Integrated DNA Technologies, Inc. (USA) and Fasmac Co., Ltd. (Japan), respectively. The optimized coding sequence for L7Ae, a ribosomal protein derived from *Archaeoglobus fulgidus*, was synthesized by GenScript, Inc. (Japan). A sequence of PSD with the FLAG tag in the C-terminal was prepared using PCR [16]. The PSD-FLAG coding sequence or L7Ae sequence was subcloned into the EcoRI/NotI or EcoRI/XhoI site of the pGEX-6p-2 vector, respectively, and transformed into *Escherichia coli* BL21 (DE3) pLysS cells. The cells were cultured in 100 mL of Luria Bertani (LB) medium (containing 100 $\mu\text{g}/\text{mL}$ ampicillin sodium) and grown until $\text{OD}_{600\text{nm}}$ was approximately 0.5. Isopropyl- β -D(-)-thiogalactopyranoside (IPTG) (Wako Pure Chemical Industries, Ltd., Japan) with a final

concentration of 1 mM was added to the medium, which was then incubated at 37°C for 3 h. After centrifugation at $3,000 \times g$ for 15 min at 4°C, the culture medium was re-suspended in Sonication buffer [50 mM Tris-HCl (pH 7.5), 150 mM NaCl, 10 mM DTT, and protease inhibitor cocktail], and the PSD or L7Ae protein was extracted from *E. coli* by sonication. Glutathione sepharoseTM 4B was used to purify PSD from the extracted solution. The amount of PSD was estimated by measuring the protein concentration using the Bradford assay.

1.1.2.6. Characterization of PSD protein composition

The composition of PSD protein was confirmed using SDS-PAGE for protein staining and western blot analysis, as previously described [12,24,25].

1.1.2.7. Liposome preparation

PS-rich liposomes were prepared using a thin film hydration method, as previously described [10,11]. Briefly, PS-rich liposomes composed of DSPC:DOPS:cholesterol at a molar ratio of 5:1:4 were extruded through polycarbonate membranes of 1 μm pore size using a mini-extruder device (Avanti Polar Lipids) [11]. The mean diameter \pm standard deviation (SD) and the mean zeta potential \pm SD were 591.7 ± 9.7 nm and -78.5 ± 0.6 mV, respectively. The liposomes were stored at 4°C until use.

1.1.2.8. Flow cytometry assay

To detect PS exposure on liposomes, aliquoted PS-rich liposomes were incubated with purified PSD at final concentrations of 0, 20, 60, and 200 $\mu\text{g}/\text{mL}$ for 3 h at 37°C. The liposomes were then centrifuged at $10,000 \times g$ for 5 min to remove the excess PSD in the supernatants, re-suspended in 100 μL of HEPES buffer [10 mM HEPES (pH 7.4), 140 mM NaCl, and 2.5 mM CaCl_2], and incubated with FITC-labeled annexin V (1:20 dilution; BioLegend, USA). After centrifugation and removal of the supernatants, the fluorescent-labeled liposomes were re-suspended in 200 μL of HEPES buffer, and fluorescence was detected using a GalliosTM flow cytometer (Beckman Coulter, USA). The data were analyzed using Kaluza software (version 1.0, Beckman Coulter).

1.1.2.9. Treatment of sEVs with PSD or L7Ae

gLuc-Lamp2c-labeled sEVs were incubated with or without PSD or L7Ae at a final concentration of 200 $\mu\text{g}/\text{mL}$ for 3 h at 37°C. The PSD or L7Ae mixtures were then washed once by ultracentrifugation at $100,000 \times g$ for 1 h to remove excess PSD. The final sEV

pellet was re-suspended in 100 μ L of PBS and used for downstream analysis.

1.1.2.10. Characterization of physicochemical properties of sEVs

The morphologies, particle sizes, and surface charges of sEV samples were evaluated as described in previous reports [16,23,25], using transmission electron microscopy (TEM; Hitachi H-7650, Hitachi High-Technologies Corporation, Japan), a qNano instrument (Izon Science Ltd., New Zealand), and a Zetasizer Nano ZS (Malvern Instruments, UK), respectively.

1.1.2.11. Affinity capture of PS⁽⁺⁾ sEVs using TIM4-conjugated beads

To isolate PS⁽⁻⁾ sEVs from sEV samples, TIM4-conjugated beads (Wako FUJIFILM, Japan) were incubated with the samples for 1 h, and the supernatants were collected as previously described [12].

1.1.2.12. Blood clearance

sEV samples were injected into the tail veins of BALB/c mice. Blood samples were collected at the indicated time points. Serum was obtained by centrifuging clotted whole blood samples at $8,000 \times g$ for 20 min at 4°C. The serum was diluted with PBS, and gLuc enzyme activity was measured using a PicaGene Dual Sea Pansy Luminescence Kit (Toyo Inc., Japan). The amount of sEVs in each sample was normalized to the injected dose (ID) and expressed as % ID/mL [10–12,16].

The half-life ($t_{1/2\alpha}$), the area under the curve (AUC), mean residence time (MRT), and clearance (CL) of gLuc-labeled sEVs from blood after intravenous (i.v.) injection in mice were calculated for each animal by integration from 5 to 240 min.

1.1.2.13. Statistical analysis

Statistical significance in the differences between two groups and multiple groups were evaluated using the Student's *t*-test and Tukey-Kramer test, respectively.

1.1.3. Results

1.1.3.1. PSD-coding pDNA was constructed and PSD protein was successfully purified

PSD-coding pDNA was newly constructed. PSD protein was extracted from BL21 (DE3) pLysS cells transfected with PSD-coding pDNA and purified using the glutathione

S-transferase purification method. To confirm that the purification was successful, the protein composition of PSD was evaluated using SDS-PAGE. The molecular weight of the designed PSD protein was 71 kDa; two bands were observed at that position, and were presumed to be derived from PSD protein (Fig. 1B). The level of expression of FLAG increased in the solution extracted from IPTG-stimulated cells (Fig. 1B). These results indicated that the desired PSD protein was successfully purified.

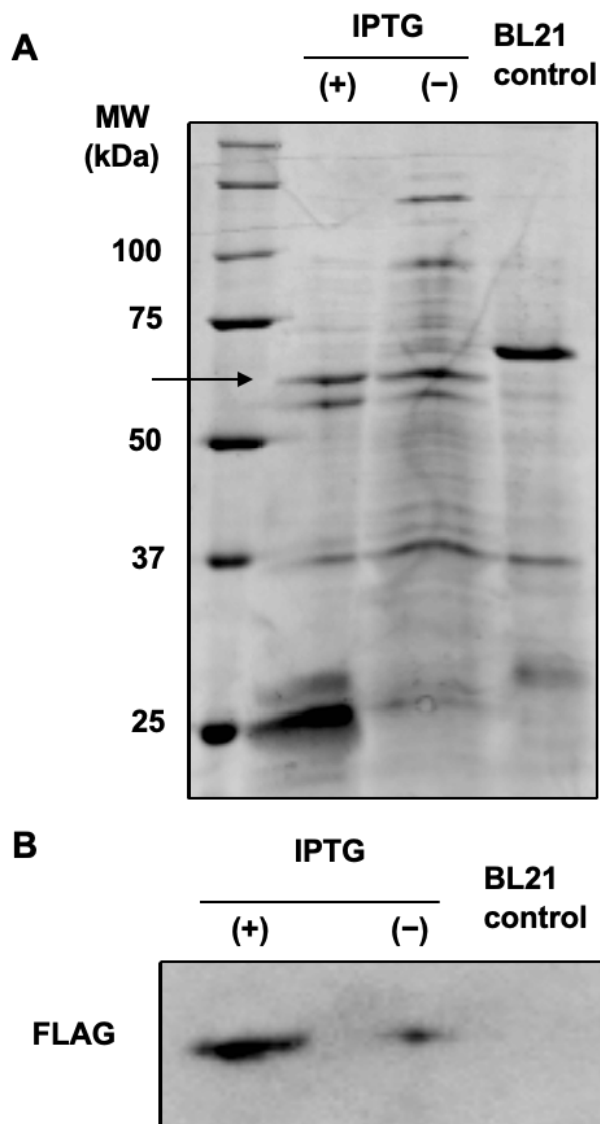


Fig. 1 Confirmation of PSD protein composition. (A) Protein profiles of PSD. Lane 1: Marker. Lane 2: Purified protein from cells cultured with IPTG. Lane 3: Purified protein from cells cultured without IPTG. Lane 4: Purified protein from non-expressing cells. (B) Western blot analysis of FLAG in purified PSD and control samples (1 μ g protein/lane).

1.1.3.2. Purified PSD protein exhibited enzyme activity

To assess whether purified PSD protein retained enzyme activity, PS-rich liposomes were used because they can be produced in large quantities and the amount of PS can be easily detected. The changes in the levels of exposed PS on PS-rich liposomes incubated with PSD were evaluated. Treatment with PSD reduced the levels of surface PS on liposomes in a concentration-dependent manner (Fig. 2A). Moreover, to confirm whether the upper peak that appears at higher concentrations of PSD is due to the formation of liposome aggregates, the relationship between forward scatter intensity, which reflects particle size, and fluorescent intensity was analyzed (Fig. 2B). The results showed an increase in size consistent with the upper peak in Fig. 2A.

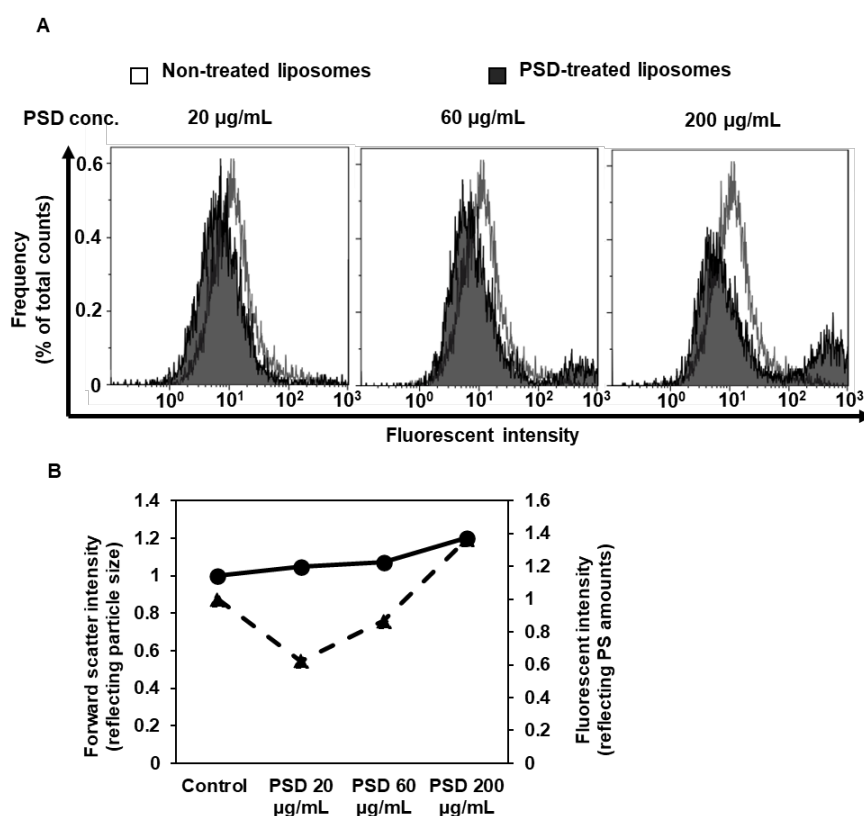


Fig. 2 Evaluation of PSD enzyme activity and liposomes size.

(A) Detection of PS exposure on liposomes incubated with various concentrations of PSD using flow cytometry analysis. (B) Geometric mean of the forward scattering intensity reflecting the particle size (solid line, circle symbols) and the fluorescence intensity reflecting the PS amounts (dotted line, triangular symbols) in the histogram in (A).

1.1.3.3. PSD-treated sEVs were identified as PS⁽⁻⁾ sEV-enriched subpopulation

The depletion of exposed PS on gLuc-Lamp2c-labeled sEVs treated with PSD was evaluated. Non-treated or PSD-treated sEVs did not exhibit morphological changes and aggregation (Figs. 3A and 3B). Western blot analysis confirmed the successful removal of excess PSD protein from the PSD-treated sEVs following the ultracentrifugation step (Fig. 3C).

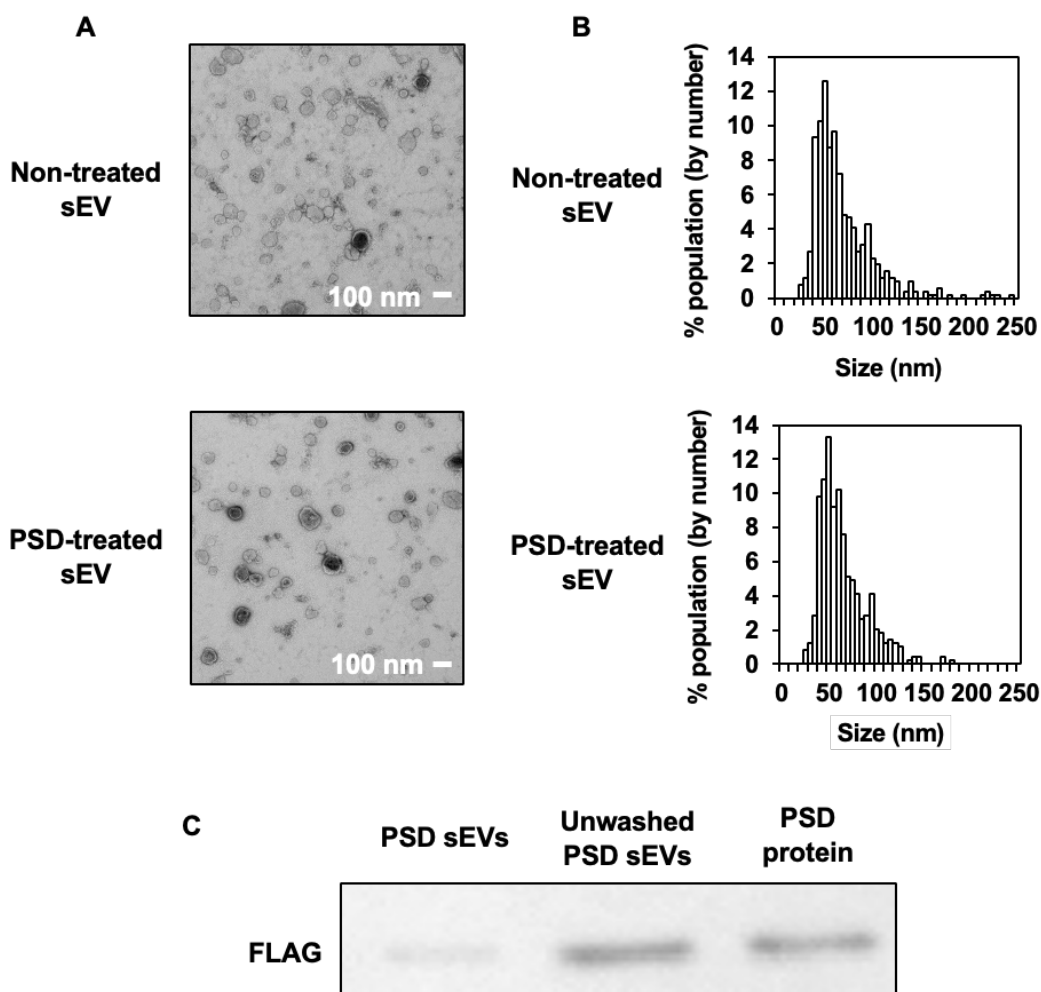


Fig. 3 Physicochemical characterization of non-treated or PSD-treated sEVs.

(A) TEM image of non-treated (top) or PSD-treated (bottom) sEVs. (B) Particle size distribution of non-treated (top) or PSD-treated (bottom) sEVs obtained by analyzing TEM images. (C) Western blot analysis of FLAG in washed or unwashed sEVs treated with PSD (1 μ g protein/lane).

TIM4-based affinity capturing was performed to quantify the PS on sEVs treated with PSD. The recovered gLuc activity in the non-captured fraction (NCF) of PSD-treated sEVs normalized to the input was approximately three times higher compared to that of non-treated sEVs (Fig. 4A).

Moreover, to confirm whether the increase in NCF was due to enzymatic conversion of PSD, sEVs were collected after treatment with another recombinant protein L7Ae. Here, L7Ae protein which is a ribosomal protein and has no enzymatic activity was used as a control group for PSD [26]. Then, NCF of non-treated or L7Ae-treated sEVs was recovered (Fig. 4B). Compared with non-treatment, the amount of NCF after L7Ae protein treatment was not increased. These results indicated that the population of PS⁽⁻⁾-sEVs have increased with the enzymatic treatment of PSD.

On the other hand, measurement of zeta potential of non-treated, PSD-treated or L7Ae-treated sEVs were -20.3 ± 2.2 , -18.2 ± 2.0 and -20.6 ± 2.2 mV, respectively. This indicated PSD treatment may not have converted enough PS to change the zeta potential of bulk sEVs.

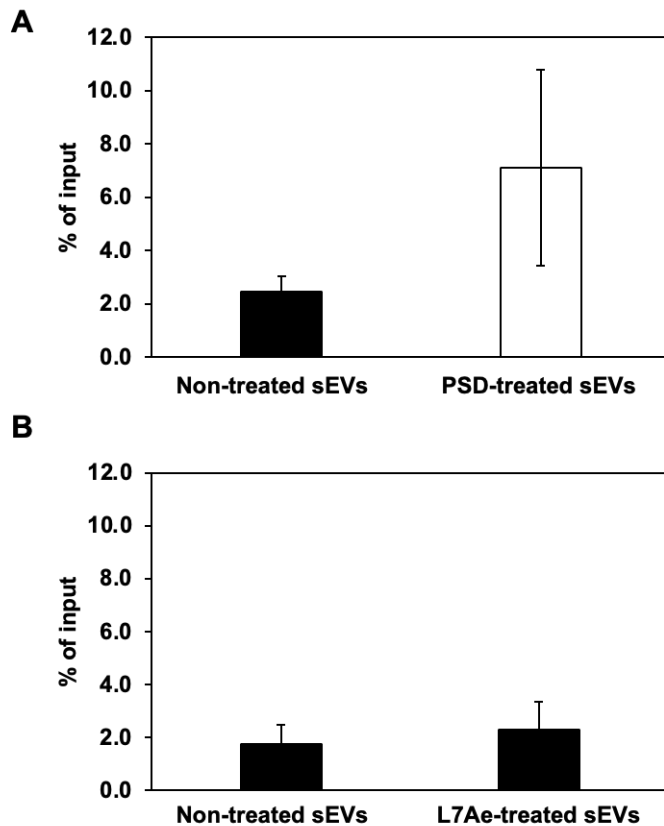


Fig. 4 Effect of NCF recovery on recombinant protein PSD or L7Ae treatment.

(A) Percentage of recovered gLuc activity in NCF of non-treated and PSD-treated sEVs using TIM4 beads. (B) Percentage recovered gLuc activity in NCF of non-treated and L7Ae-treated sEVs using TIM4 beads. Results are expressed as mean \pm SD ($n = 3$).

1.1.3.4. PS⁽⁻⁾ sEVs recovered from PSD-treated bulk sEVs showed long blood-circulation periods

The serum concentration profile and PK parameters of the NCF of PSD-treated sEVs after i.v. administration were evaluated. The NCF of PSD-treated sEVs circulated longer in blood than bulk non-treated sEVs (Fig. 5). In addition, the half-life and the AUC of PSD-treated sEVs NCF were significantly larger, whereas the CL of that were significantly smaller than those of bulk non-treated sEVs (Table 1).

These results indicated that the treatment of sEVs with PSD successfully increased the yield of PS⁽⁻⁾ sEVs with long blood-circulation half-life.

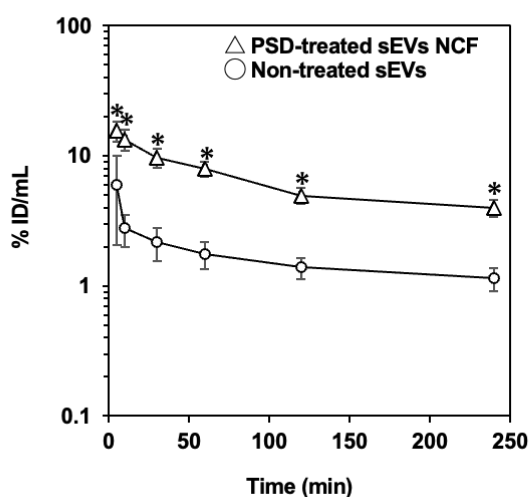


Fig. 5 Pharmacokinetic characterization of PSD-treated sEVs.

Time course of serum concentrations of gLuc activity after intravenous administration of non-treated sEVs (3×10^8 RLU/s/shot) or NCF of PSD-treated sEVs (1×10^8 RLU/s/shot) into mice. Results are expressed as mean % ID/mL \pm SD ($n = 3$). * $p < 0.05$ compared with non-treated sEVs.

Table 1 Pharmacokinetic parameters of non-treated sEVs and NCF of PSD-treated sEVs after intravenous administration into mice.

Results are expressed as mean \pm SD ($n = 3$). * $p < 0.05$ compared with non-treated sEVs.

Sample	$t_{1/2\alpha}$ (min)	AUC (% ID·h/mL)	CL (mL/h)	MRT (h)
PSD-treated sEVs NCF	$36.6 \pm 9.1^*$	$24.8 \pm 3.5^*$	$4.1 \pm 0.6^*$	1.49 ± 0.06
Non-treated sEVs	16.3 ± 8.0	6.3 ± 1.2	16.3 ± 3.1	1.49 ± 0.21

1.1.4. Discussion

Establishment of preparation methods for massive quantities of sEVs along with PK evaluation is pivotal for the success of sEV translational applications. The previous report indicated that PS⁽⁻⁾ sEVs are promising drug carriers, owing to their long blood circulation periods and high biocompatibility [12]. However, the currently used PS⁽⁻⁾ sEV isolation method is unsuitable for large-scale preparation because of its high cost, poor scalability, and limited yield. Herein, I proposed a distinct approach for the efficient preparation of PS⁽⁻⁾ sEVs: the manipulation of lipid composition using PSD [23,27]. In this study, I developed a method for the efficient preparation of PS⁽⁻⁾ sEVs using PSD, a mitochondrial enzyme that converts PS into PE [22]. Since it has been reported that 70% of exposed PS on PS-rich liposomes can be transformed into PE [27], I hypothesized that PSD can partly transform PS⁽⁺⁾ sEVs into PS⁽⁻⁾ sEVs with their cargoes biologically intact via an enzymatic reaction, which results in increased yields of PS⁽⁻⁾ sEVs.

A weaker fluorescence signal of Annexin V, which is specific to PS, was detected after the co-incubation of PS-rich liposomes with PSD. This result suggests that the PSD protein exerted enzyme activity that reduced the amount of surface PS. The upper peak observed at higher concentrations of PSD was presumed to indicate an increase in the apparent liposome size, likely due to the formation of liposome aggregates. This was suggested by the increase in the geometric mean of forward scatter in the PSD-treated group. Similarly, in the case of sEVs, the formation of sEV aggregates may occur due to PSD treatment as well as PS-rich liposomes.

PSD treatment could also be applied to the depletion of PS exposed on sEV outer-leaflet membranes; this was confirmed by the change in the population size of PS⁽⁻⁾ sEVs and the serum concentration profile. As PSD-treated sEVs were found to comprise a PS⁽⁻⁾ sEV-enriched subpopulation, the surface charge was considered to have been changed by PSD treatment. To further confirm that the effect was not due to recombinant protein, we utilized another recombinant protein L7Ae, which was purified the same procedure as PSD protein. The amount of PS⁽⁻⁾ sEVs recovered from L7Ae-treated bulk sEVs was similar to that of non-treated. These results suggest that PSD treatment increases the amount of PS⁽⁻⁾ sEVs through enzymatic conversion. However, PSD-treated sEVs showed a negative charge comparable to that of non-treated or L7Ae-treated sEVs. It was assumed that the increase in the population of PS⁽⁻⁾ sEV population among PSD-treated sEVs was insufficient to alter the zeta potential. The limited effect of PSD treatment may be due to limited access to the surface by membrane proteins and glycans of sEVs. Furthermore, some studies have reported that the activity of the PSD enzyme depends on the reaction solution or PS concentration [28–30]. Hence, the limited efficiency of enzymatic PS

depletion should be improved in future studies.

1.1.5. Summary of Section 1

In this section, I successfully increased the PS⁽⁻⁾ sEV yield from cultured cell-derived sEVs using PSD treatment. This approach to improve the productivity of PS⁽⁻⁾ sEVs based on PSD treatment, as well as the basic PK information, will be foundational for the therapeutic application of PS⁽⁻⁾ sEVs.

Section 2

Development of a detection method for a subpopulation focusing on PS status in small extracellular vesicles

In section 1, I successfully increased the productivity of PS⁽⁻⁾ sEVs, which can contribute to the application of PS⁽⁻⁾ sEV based formulations. In previous studies, quality control of the formulation has been deemed crucial to ensure its therapeutic efficacy, such as stability and potency [31–33]. In the case of PS⁽⁻⁾ sEV-based formulation, it would be crucial to detect PS⁽⁻⁾ sEVs population in bulk sEVs for evaluate the quality of the formulation. Next, for quality control toward PS⁽⁻⁾ sEV-based formulation, I attempted to develop a labeling method to detect PS⁽⁻⁾ sEVs from the bulk.

To qualitatively detect sEVs, fluorescent labeling was used. Fluorescent labeling has the advantages of simple detection by microscopy and in performing multicolor analysis [34]. Fluorescent labeling of sEVs using lipophilic dyes such as DiI and PKH dye, which can label a wide range of sEVs, is restricted to single use [35–38]. Multicolor analysis is necessary to detect target sEV population in bulk sEVs.

In this study, I designed two fusion proteins comprising fluorescent proteins and sEV-tropic protein or peptide to enable multicolor analysis. One fusion protein consists of lactoadherin (LA) protein, a PS-binding protein, and EGFP (EGFP-LA) to detect PS-positive sEVs [39–41]. The other fusion protein incorporates the Vn96 peptide, which exhibits an affinity for the sEV-lipid membrane, and mCherry (mCherry-Vn96) to detect bulk sEVs [42,43]. I attempted to develop a simple method for detecting sEVs according to PS-expression levels on the surface of sEVs using these two fusion proteins.

Bulk sEVs were isolated from the culture supernatant of B16-BL6 cells double-transfected with plasmid DNAs encoding EGFP-LA and mCherry-Vn96 by ultracentrifugation method. Fluorescence from both fusion proteins was observed in bulk sEVs using fluorescence microscopy. Additionally, in PS⁽⁺⁾ sEV-depleted fraction isolated from bulk sEVs by TIM4 affinity beads, the fluorescent signals of EGFP-LA were decreased and the predominant fluorescent signals were from mCherry-Vn96. The result of image analysis revealed that both signals were mostly detected in bulk sEVs, but single fluorescent signals of mCherry-Vn96 were also detected to some extent, which imply the existence of PS⁽⁻⁾ sEVs in bulk sEVs. The physicochemical properties of sEVs labeled with these fusion proteins were hardly altered compared to non-labeled sEVs.

In this section, I developed a qualitative detection method using two types of fusion protein consisting of fluorescent protein. This method could label sEVs and could detect

differences in fluorescence distribution of sEVs. Consequently, this method allowed for easy qualitative analysis for PS⁽⁻⁾ sEV subpopulation by fluorescence microscopy, suggesting that this method can be useful for quality check for PS⁽⁻⁾ sEVs based formulation.

Chapter 2

Evaluation of the effect of extracellular vesicles particle size on the permeability of extracellular vesicles in the gastrointestinal tract

Oral formulations are a non-invasive and convenient route of administration for patients compared to injectable formulations. To date, various nanoparticles have been studied for application as drug delivery carriers in oral formulations [44]. In recent years, several reports have demonstrated the pharmacological effects of orally administered sEVs, including anti-tumor and anti-inflammatory effects [45,46]. PK analysis of EVs is important for the development of EVs into oral formulations. For oral administration, the most important factors affecting pharmacokinetics are biological barriers in the GI tract such as the gastrointestinal mucosa, tight junctions and the mononuclear phagocytic system [44]. Nanoparticle size is crucial for PK improvement, with smaller sizes potentially enhancing permeability across barriers [13,15,47,48]. Thus, I hypothesized that smaller EVs could enhance GI tract permeability.

In this study, three different sizes of EVs were isolated from cell culture medium by differential centrifugation and size exclusion chromatography. After intraduodenal administration of these EVs, the effect of EV size on absorption efficiency and distribution of EVs in the GI tract was evaluated. To evaluate absorption efficiency, I used a fusion protein (Gag-gLuc) composed of EV-tropic protein (Gag) and *Gaussia* luciferase (gLuc) to label EVs. After intraduodenal administration of each labeled EV, gLuc activity in serum, small intestine and liver was measured to evaluate *in vivo* absorption efficiency of each EV. Moreover, to identify recipient cell types of EVs in GI tract, mice were subjected to intraduodenal administration of EV samples labeled with fluorescent dye.

Three types of EVs with different size were successfully isolated from B16-BL6 cell culture medium. From the TEM images of these EVs, the EVs isolated were approximately 30, 100, and 500 nm in diameter. In the group of mice intraduodenally administered with EVs of all sizes, little luciferase activity was detected in both serum and organs. Moreover, immunohistochemical analysis was also performed on sections of small intestine and liver after intraduodenal administration of fluorescently labeled EVs. In the intestine sections in all groups administered with EVs, co-localization of EVs and F4/80 as a macrophage marker was observed in the intestinal lamina propria. This co-localization tended to increase in the group of mice that received smaller EVs. On the other hand, co-localization of EVs and CD31 as an endothelial marker hardly observed in the intestine. These results indicate that EVs in the GI tract are taken up by macrophages in the intestinal lamina propria and hardly translocated into the blood.

In this chapter, I hypothesized that smaller EVs would exhibit higher permeability in the GI tract after intraduodenal administration. Contrary to expectations, all types of EVs with different size showed poor absorption into the systemic circulation and were instead

taken up by immune cells such as macrophages in the intestinal lamina propria. These findings can be a key for the application of EVs in oral immunotherapy.

Conclusion

EVs are expected for application as DDS carrier, which have advantages on high biocompatibility, loading exogenous molecules by genetic engineering. Therefore, EV formulations are desired, but it is desirable to EV-based formulation with superior PK. The purpose of this study is a basic investigation for the development of EV-based formulations, focusing on the effects of size and surface charge on the PK of EVs.

In section 1 of chapter 1, I successfully increased productivity of PS⁽⁻⁾ sEVs using PSD protein without changing PK properties of PS⁽⁻⁾ sEVs.

In section 2, I successfully detected PS⁽⁻⁾ sEVs in bulk sEVs using fluorescence microscope and two types of fluorescent fusion proteins.

In chapter 2, I found that all sizes of EVs were trapped by macrophages in the intestinal lamina propria instead of transferred to blood. I also found that the smaller EVs of size were more taken up by macrophages.

The findings in this thesis contribute to the development of EV subpopulation-based formulation with improved pharmacokinetic properties of EVs.

List of publications included in this thesis

Development of Enzymatic Depletion Methods for Preparation of Small Extracellular Vesicles with Long Blood-Circulation Half-Life.

Pharm Res. 2023 Apr;40(4):855-861,

Development of a Simple Labeling Method using Fluorescent Protein Fusion Proteins Targeting Membrane Lipids of Small Extracellular Vesicles.

Manuscript in preparation

Investigation of *In Vivo* Behavior of Extracellular Vesicles with Different Sizes after Intraduodenal Administration.

Manuscript in preparation

Acknowledgements

First and foremost, I would like to express my deepest gratitude to former Professor Yoshinobu Takakura, Ph.D. from the Department of Biopharmaceutics and Drug Metabolism, Graduate School of Pharmaceutical Science, Kyoto University for accepting me from Kyoto Pharmaceutical University as his student and giving me the opportunity to meet so brilliant people in this laboratory and external communities.

Then, I would also like to express my deepest gratitude to Associate professor Yuki Takahashi, Ph.D. from the Department of Biopharmaceutics and Drug Metabolism, Graduate School of Pharmaceutical Science. His passion for research has inspired all members including me in this laboratory, and his extensive knowledge and patient guidance assisted me in completing my thesis. Under Dr. Takahashi's instructions, I gained stimulatory discussion and ability to explore the subject, complete experiments, and so on.

Then, I would like to gratitude to current Professor Yuriko, Higuchi, Ph.D. from the Department of Biopharmaceutics and Drug Metabolism, Graduate School of Pharmaceutical Science, Kyoto University for accepting me from Kyoto Pharmaceutical University for precious discussion and her critical advice.

I would like to thank all members of the the Department of Biopharmaceutics and Drug Metabolism, both the alumni and current members, for fruitful discussion, memorable memories and their help with my life and experiments. I would like to give my special thanks to Ms. Noriko Hikihara, Dr. Aki Yamamoto, Mr. Shimpei Kitamura, Ms. Ayane Yabuta, Ms. Momoko Naiki, Ms. Saori Sakagami, Mr. Hiroto Otera and Ms. Anna Taniwaki for their unstinting help.

Last but not least, I would like to express my utmost gratitude to my family for raising me, providing me with opportunity to persue a path to pharmaceutical science and continuous support to study and pursue my aspirations throughout my life.

References

1. Jeppesen DK, Zhang Q, Franklin JL, Coffey RJ. Extracellular vesicles and nanoparticles: emerging complexities. *Trends Cell Biol.* 2023;33:667–81.
2. van Niel G, D'Angelo G, Raposo G. Shedding light on the cell biology of extracellular vesicles. *Nat Rev Mol Cell Biol.* 2018;19:213–28.
3. Raposo G, Stoorvogel W. Extracellular vesicles: exosomes, microvesicles, and friends. *J Cell Biol.* 2013;200:373–83.
4. Yáñez-Mó M, Siljander PR-M, Andreu Z, Zavec AB, Borràs FE, Buzas EI, et al. Biological properties of extracellular vesicles and their physiological functions. *J Extracell Vesicles.* 2015;4:27066.
5. Tkach M, Théry C. Communication by Extracellular Vesicles: Where We Are and Where We Need to Go. *Cell.* 2016;164:1226–32.
6. Rhim W-K, Kim JY, Lee SY, Cha S-G, Park JM, Park HJ, et al. Recent advances in extracellular vesicle engineering and its applications to regenerative medicine. *Biomater Res.* 2023;27:130.
7. Ferguson SW, Nguyen J. Exosomes as therapeutics: The implications of molecular composition and exosomal heterogeneity. *J Control Release.* 2016;228:179–90.
8. Smith ZJ, Lee C, Rojalin T, Carney RP, Hazari S, Knudson A, et al. Single exosome study reveals subpopulations distributed among cell lines with variability related to membrane content. *J Extracell Vesicles.* 2015;4:28533.
9. Yamashita T, Takahashi Y, Takakura Y. Possibility of Exosome-Based Therapeutics and Challenges in Production of Exosomes Eligible for Therapeutic Application. *Biol Pharm Bull.* 2018;41:835–42.
10. Imai T, Takahashi Y, Nishikawa M, Kato K, Morishita M, Yamashita T, et al. Macrophage-dependent clearance of systemically administered B16BL6-derived exosomes from the blood circulation in mice. *J Extracell Vesicles.* 2015;4:26238.
11. Matsumoto A, Takahashi Y, Nishikawa M, Sano K, Morishita M, Charoenviriyakul C, et al. Role of Phosphatidylserine-Derived Negative Surface Charges in the Recognition and Uptake of Intravenously Injected B16BL6-Derived Exosomes by Macrophages. *J Pharm Sci.* 2017;106:168–75.
12. Matsumoto A, Takahashi Y, Ogata K, Kitamura S, Nakagawa N, Yamamoto A, et al. Phosphatidylserine-deficient small extracellular vesicle is a major somatic cell-derived sEV subpopulation in blood. *iScience.* 2021;24:102839.
13. Ejazi SA, Louisthelmy R, Maisel K. Mechanisms of Nanoparticle Transport across

- Intestinal Tissue: An Oral Delivery Perspective. *ACS Nano*. 2023;17:13044–61.
14. Shen M-Y, Liu T-I, Yu T-W, Kv R, Chiang W-H, Tsai Y-C, et al. Hierarchically targetable polysaccharide-coated solid lipid nanoparticles as an oral chemo/thermotherapy delivery system for local treatment of colon cancer. *Biomaterials*. 2019;197:86–100.
 15. Desai MP, Labhasetwar V, Amidon GL, Levy RJ. Gastrointestinal uptake of biodegradable microparticles: effect of particle size. *Pharm Res*. 1996;13:1838–45.
 16. Takahashi Y, Nishikawa M, Shinotsuka H, Matsui Y, Ohara S, Imai T, et al. Visualization and in vivo tracking of the exosomes of murine melanoma B16-BL6 cells in mice after intravenous injection. *J Biotechnol*. 2013;165:77–84.
 17. Charoenviriyakul C, Takahashi Y, Morishita M, Nishikawa M, Takakura Y. Role of Extracellular Vesicle Surface Proteins in the Pharmacokinetics of Extracellular Vesicles. *Mol Pharm*. 2018;15:1073–80.
 18. Yamamoto A, Yasue Y, Takahashi Y, Takakura Y. Determining The Role of Surface Glycans in The Pharmacokinetics of Small Extracellular Vesicles. *J Pharm Sci*. 2021;110:3261–7.
 19. Subra C, Laulagnier K, Perret B, Record M. Exosome lipidomics unravels lipid sorting at the level of multivesicular bodies. *Biochimie*. 2007;89:205–12.
 20. Llorente A, Skotland T, Sylvänne T, Kauhanen D, Róg T, Orłowski A, et al. Molecular lipidomics of exosomes released by PC-3 prostate cancer cells. *Biochim Biophys Acta*. 2013;1831:1302–9.
 21. Matsumoto A, Takahashi Y, Chang H-Y, Wu Y-W, Yamamoto A, Ishihama Y, et al. Blood concentrations of small extracellular vesicles are determined by a balance between abundant secretion and rapid clearance. *J Extracell Vesicles*. 2020;9:1696517.
 22. Vance JE, Tasseva G. Formation and function of phosphatidylserine and phosphatidylethanolamine in mammalian cells. *Biochim Biophys Acta*. 2013;1831:543–54.
 23. Yamashita T, Takahashi Y, Nishikawa M, Takakura Y. Effect of exosome isolation methods on physicochemical properties of exosomes and clearance of exosomes from the blood circulation. *Eur J Pharm Biopharm*. 2016;98:1–8.
 24. Charoenviriyakul C, Takahashi Y, Morishita M, Matsumoto A, Nishikawa M, Takakura Y. Cell type-specific and common characteristics of exosomes derived from mouse cell lines: Yield, physicochemical properties, and pharmacokinetics. *Eur J Pharm Sci*. 2017;96:316–22.
 25. Liu W, Takahashi Y, Morishita M, Nishikawa M, Takakura Y. Development of CD40L-modified tumor small extracellular vesicles for effective induction of antitumor

- immune response. *Nanomedicine (Lond)*. 2020;15:1641–52.
26. Rozhdestvensky TS, Tang TH, Tchirkova I V, Brosius J, Bachellerie J-P, Hüttenhofer A. Binding of L7Ae protein to the K-turn of archaeal snoRNAs: a shared RNA binding motif for C/D and H/ACA box snoRNAs in Archaea. *Nucleic Acids Res*. 2003;31:869–77.
27. Drechsler C, Markones M, Choi J-Y, Frieling N, Fiedler S, Voelker DR, et al. Preparation of Asymmetric Liposomes Using a Phosphatidylserine Decarboxylase. *Biophys J*. 2018;115:1509–17.
28. Choi J-Y, Augagneur Y, Mamoun C Ben, Voelker DR. Identification of gene encoding *Plasmodium knowlesi* phosphatidylserine decarboxylase by genetic complementation in yeast and characterization of in vitro maturation of encoded enzyme. *J Biol Chem*. 2012;287:222–32.
29. Satre M, Kennedy EP. Identification of bound pyruvate essential for the activity of phosphatidylserine decarboxylase of *Escherichia coli*. *J Biol Chem*. 1978;253:479–83.
30. Drechsler C, Markones M, Choi J-Y, Frieling N, Fiedler S, Voelker DR, et al. Preparation of Asymmetric Liposomes Using a Phosphatidylserine Decarboxylase. *Biophys J*. 2018;115:1509–17.
31. Cunha S, Costa CP, Moreira JN, Sousa Lobo JM, Silva AC. Using the quality by design (QbD) approach to optimize formulations of lipid nanoparticles and nanoemulsions: A review. *Nanomedicine*. 2020;28:102206.
32. Gawin-Mikołajewicz A, Nartowski KP, Dyba AJ, Gołkowska AM, Malec K, Karolewicz B. Ophthalmic Nanoemulsions: From Composition to Technological Processes and Quality Control. *Mol Pharm*. 2021;18:3719–40.
33. Varenne F, Vauthier C. Practical Guidelines for the Characterization and Quality Control of Nanoparticles in the Pharmaceutical Industry. *Emerging Technologies for Nanoparticle Manufacturing*. Cham: Springer International Publishing; 2021. p. 487–508.
34. He Y, Xing Y, Jiang T, Wang J, Sang S, Rong H, et al. Fluorescence labeling of extracellular vesicles for diverse bio-applications in vitro and in vivo. *Chem Commun (Camb)*. 2023;59:6609–26.
35. Pužar Dominkuš P, Stenovec M, Sitar S, Lasič E, Zorec R, Plemenitaš A, et al. PKH26 labeling of extracellular vesicles: Characterization and cellular internalization of contaminating PKH26 nanoparticles. *Biochim Biophys Acta Biomembr*. 2018;1860:1350–61.
36. Dehghani M, Gulvin SM, Flax J, Gaborski TR. Systematic Evaluation of PKH Labelling on Extracellular Vesicle Size by Nanoparticle Tracking Analysis. *Sci Rep*. 2020;10:9533.

37. Santelices J, Ou M, Hui WW, Maegawa GHB, Edelman MJ. Fluorescent Labeling of Small Extracellular Vesicles (EVs) Isolated from Conditioned Media. *Bio Protoc.* 2022;12.
38. Barreca V, Boussadia Z, Polignano D, Galli L, Tirelli V, Sanchez M, et al. Metabolic labelling of a subpopulation of small extracellular vesicles using a fluorescent palmitic acid analogue. *J Extracell Vesicles.* 2023;12:e12392.
39. Andersen MH, Graversen H, Fedosov SN, Petersen TE, Rasmussen JT. Functional analyses of two cellular binding domains of bovine lactadherin. *Biochemistry.* 2000;39:6200–6.
40. Morishita M, Takahashi Y, Nishikawa M, Sano K, Kato K, Yamashita T, et al. Quantitative analysis of tissue distribution of the B16BL6-derived exosomes using a streptavidin-lactadherin fusion protein and iodine-125-labeled biotin derivative after intravenous injection in mice. *J Pharm Sci.* 2015;104:705–13.
41. Arima Y, Liu W, Takahashi Y, Nishikawa M, Takakura Y. Effects of Localization of Antigen Proteins in Antigen-Loaded Exosomes on Efficiency of Antigen Presentation. *Mol Pharm.* 2019;16:2309–14.
42. Ghosh A, Davey M, Chute IC, Griffiths SG, Lewis S, Chacko S, et al. Rapid isolation of extracellular vesicles from cell culture and biological fluids using a synthetic peptide with specific affinity for heat shock proteins. *PLoS One.* 2014;9:e110443.
43. Bijnsdorp I V, Maxouri O, Kardar A, Schelfhorst T, Piersma SR, Pham T V, et al. Feasibility of urinary extracellular vesicle proteome profiling using a robust and simple, clinically applicable isolation method. *J Extracell Vesicles.* 2017;6:1313091.
44. Hodayun B, Lin X, Choi H-J. Challenges and Recent Progress in Oral Drug Delivery Systems for Biopharmaceuticals. *Pharmaceutics.* 2019;11.
45. Agrawal AK, Aqil F, Jeyabalan J, Spencer WA, Beck J, Gachuki BW, et al. Milk-derived exosomes for oral delivery of paclitaxel. *Nanomedicine.* 2017;13:1627–36.
46. Arntz OJ, Pieters BCH, Oliveira MC, Broeren MGA, Bennink MB, de Vries M, et al. Oral administration of bovine milk derived extracellular vesicles attenuates arthritis in two mouse models. *Mol Nutr Food Res.* 2015;59:1701–12.
47. Yao M, He L, McClements DJ, Xiao H. Uptake of Gold Nanoparticles by Intestinal Epithelial Cells: Impact of Particle Size on Their Absorption, Accumulation, and Toxicity. *J Agric Food Chem.* 2015;63:8044–9.
48. Jia L, Wong H, Cerna C, Weitman SD. Effect of nanonization on absorption of 301029: ex vivo and in vivo pharmacokinetic correlations determined by liquid chromatography/mass spectrometry. *Pharm Res.* 2002;19:1091–6.